ELSEVIER

Neurobiology of Aging 30 (2009) 241–256

NEUROBIOLOGY OF AGING

www.elsevier.com/locate/neuaging

Deregulation of NMDA-receptor function and down-stream signaling in APP[V717I] transgenic mice

I. Dewachter[a,1], R.K. Filipkowski[b,1], C. Priller[c,1], L. Ris[e], J. Neyton[d], S. Croes[a], D. Terwel[a], M. Gysemans[f], H. Devijver[a], P. Borghgraef[a], E. Godaux[e], L. Kaczmarek[b], J. Herms[c], F. Van Leuven[a,*]

[a] *Experimental Genetics Group, LEGT_EGG, K.U.Leuven, Campus Gasthuisberg ON1-06.602, 3000 Leuven, Belgium*
[b] *Laboratory of Molecular Neurobiology, Nencki Institute, Warsawa, Poland*
[c] *Department of Neuropathology, Ludwig-Maximilians-Universität Muenich, Muenich, Germany*
[d] *Laboratoire de Neurobiologie, CNRS UMR 8544 Ecole Normale Superieure, Paris, France*
[e] *Université de Mons-Hainaut, Faculté de Medecine et Pharmacie, 7000 Mons, Belgium*
[f] *Laboratory of Solid State Physics and Magnetism, K.U.Leuven, 3000 Leuven, Belgium*

Received 16 April 2007; received in revised form 13 June 2007; accepted 15 June 2007
Available online 27 July 2007

Abstract

Evidence is accumulating for a role for amyloid peptides in impaired synaptic plasticity and cognition, while the underlying mechanisms remain unclear. We here analyzed the effects of amyloid peptides on NMDA-receptor function in vitro and in vivo. A synthetic amyloid peptide preparation containing monomeric and oligomeric Aβ (1-42) peptides was used and demonstrated to bind to synapses expressing NMDA-receptors in cultured hippocampal and cortical neurons. Pre-incubation of primary neuronal cultures with Aβ peptides significantly inhibited NMDA-receptor function, albeit not by a direct pharmacological inhibition of NMDA-receptors, since acute application of Aβ peptides did not change NMDA-receptor currents in autaptic hippocampal cultures nor in xenopus oocytes expressing recombinant NMDA-receptors. Pre-incubation of primary neuronal cultures with Aβ peptides however decreased NR2B-immunoreactive synaptic spines and surface expression of NR2B containing NMDA-receptors. Furthermore, we extended these findings for the first time in vivo, demonstrating decreased concentrations of NMDA-receptor subunit NR2B and PSD-95 as well as activated α-CaMKII in postsynaptic density preparations of APP[V717I] transgenic mice. This was associated with impaired NMDA-dependent LTP and decreased NMDA- and AMPA-receptor currents in hippocampal CA1 region in APP[V717I] transgenic mice. In addition, induction of c-Fos following cued and contextual fear conditioning was significantly impaired in the basolateral amygdala and hippocampus of APP[V717I] transgenic mice. Our data demonstrate defects in NMDA-receptor function and learning dependent signaling cascades in vivo in APP[V717I] transgenic mice and point to decreased surface expression of NMDA-receptors as a mechanism involved in early synaptic defects in APP[V717I] transgenic mice in vivo.
© 2007 Elsevier Inc. All rights reserved.

Keywords: NMDA-receptor; Oligomeric; Amyloid peptides; APP transgenic mice; Synaptic plasticity; c-Fos

1. Introduction

In Alzheimer's Disease research, emphasis is shifting towards the study of the early phases of the disease also referred to as "mild cognitive impairment", based on the hope that the disease could be reversible at this point. The "early" stages are characterized by subtle cognitive dysfunction in the absence of neuronal loss, a condition well mimicked by APP transgenic mice. A central role for amyloid peptides in early synaptic dysfunction and cognition is gaining experimental support (Lambert et al., 1998; Moechars et al., 1999; Dewachter et al., 2002; Postina et al., 2004; Dodart et al.,

* Corresponding author. Tel.: +32 16 34 58 88; fax: +32 16 34 58 71.
E-mail address: fredvl@med.kuleuven.be (F. Van Leuven).
[1] Authors contributed equally.

0197-4580/$ – see front matter © 2007 Elsevier Inc. All rights reserved.
doi:10.1016/j.neurobiolaging.2007.06.011

2002; Cleary et al., 2005; Klyubin et al., 2005; Puzzo et al., 2005; Walsh et al., 2005a,b; Lesne et al., 2006; Gong et al., 2006; Snyder et al., 2005, for reviews see Selkoe, 2002; Walsh and Selkoe, 2004; Walsh et al., 2005a,b; Small et al., 2001; Small, 2004). Nevertheless, the molecular mechanisms underlying the synaptic dysfunction remain to be resolved in vivo.

Transgenic mice that overexpress mutant APP display early deficits in synaptic plasticity and memory, even before developing the typical AD pathology, which progressively worsens with age (Moechars et al., 1999; Chapman et al., 1999; Dewachter et al., 2002; Oddo et al., 2003). We previously demonstrated that deficits in LTP in the hippocampal CA1 region and cognitive defects in APP[V717I] transgenic mice can be rescued by inhibiting amyloid peptide production (Moechars et al., 1999; Postina et al., 2004). Because these deficits precede the development of senile plaques and amyloid angiopathy, the high-molecular weight fibrillar amyloid peptides cannot be the trigger (Moechars et al., 1999). Instead, amyloid derived diffusible ligands (ADDLs) or oligomeric amyloid peptides are more and more considered the predominant species interfering with neuronal activities and particularly with LTP (Walsh et al., 2002, 2005a,b). ADDLs and oligomeric amyloid peptides accumulate in AD brain (Gong et al., 2003) as well as in brain of APP transgenic mice (Lesne et al., 2006; Oddo et al., 2003). ADDLs bind to a subset of synaptic terminals (Lacor et al., 2004) and incubation of oligomeric amyloid peptides during ~60 min disrupts LTP (Lambert et al., 1998; Wang et al., 2002). Elegant in vitro studies have recently demonstrated that amyloid peptides can affect synapse composition and structure (Lacor et al., 2007) and can drive loss of surface glutamate receptors, i.e. NMDA- and AMPA-receptors (Snyder et al., 2005; Almeida et al., 2005; Hsieh et al., 2006; Goto et al., 2006; Lacor et al., 2007), mechanisms that potentially underlay defects in synaptic plasticity and eventually synaptic loss (Hsieh et al., 2006; Shankar et al., 2007). Whether amyloid peptides can cause a direct pharmacological inhibition of NMDA-receptor currents, and the molecular mechanisms of early synaptic plasticity in vivo in APP transgenic mice remain to be further resolved.

In this work, we addressed these questions to contribute to our understanding of the role of amyloid peptides on synaptic defects and particularly NMDA-receptor function in vitro and in vivo, in APP[V717I] transgenic mice. We demonstrate that a synthetic amyloid peptide preparation containing monomeric and oligomeric but not fibrillar amyloid peptides, bound to synapses expressing NR2B containing NMDA-receptors in cultured hippocampal and cortical neurons. Pre-incubation of primary neurons with this amyloid peptide preparation significantly attenuated NMDA-mediated increase of cytosolic calcium, in contrast acute application of Aβ peptides did not change NMDA-receptor currents in autaptic hippocampal cultures nor in xenopus oocytes expressing recombinant NMDA-receptors. This indicates that Aβ peptides affected NMDA-receptor function, but not by a direct pharmacological modulation of the receptors. Pre-incubation of primary neurons with the amyloid peptide preparation however decreased NR2B-immunoreactive spine density and surface expression of NR2B. We further extended our findings to the in vivo situation and demonstrate colocalization of amyloid peptides and NMDA-receptors in stratum radiatum of hippocampal CA1 region. In addition, postsynaptic concentrations of NR2B and PSD-95 were significantly decreased in brain of APP[V717I] transgenic mice. This correlated with impaired NMDA-dependent LTP and decreased NMDA-receptor activation in hippocampal CA1 region in APP[V717I] transgenic mice. Furthermore, NMDA-dependent signaling cascades involved in learning and memory were impaired, reflected in decreased concentrations of activated α-CaMKII in postsynaptic densities in APP[V717I] transgenic mice, and decreased induction of c-Fos following fear conditioning in APP[V717I] transgenic mice. Our data gain insight in the mechanisms involved in vitro and in vivo, in amyloid induced synaptic dysfunction, deregulation of NMDA-receptor function and downstream signaling cascades involved in learning in memory.

2. Materials and methods

2.1. Mice

The generation and basic characterization of transgenic APP[V717I] mice used in this study, has been described previously (Moechars et al., 1999). These mice overexpress human mutant APP[V717I] under control of the mouse Thy1 gene promoter warranting neuron-specific and postnatal expression of the transgene. The mice display memory deficits before robust amyloid pathology develops (Moechars et al., 1999; Van Dorpe et al., 2000; Dewachter et al., 2002). For colocalization studies of amyloid peptides and NR2B, double transgenic mice, co-expressing APPV717I and PS1A246E (APP[V717I] × PS1[A246E] transgenic mice) both under control of the Thy1 gene promoter were used, displaying higher concentrations of Aβ (1-42) peptides as compared to single APP[V717I] transgenic mice. Generation and characterization of PS1[A246E] transgenic mice has been described previously (Dewachter et al., 2000, 2007). All experimental procedures were performed in accordance with the regulations of, and authorized by the Ethical Commission for Animal Experimentation of the K.U.Leuven.

2.2. Aβ (1-42) oligomer ($A\beta_{oligo}$) and fibril formation

2.2.1. Initial solubilization of Aβ peptide

Aβ (1-42) peptides (Bachem) were resuspended in 1,1,1,3,3,3-hexafluoro-2-propanol (HFIP; H8508; Sigma) 100% HFIP to 1 mM and then aliquoted in centrifuge tubes. The HFIP was allowed to evaporate in the fume hood, and the resulting clear peptide films were dried under vacuum and stored desiccated at −20 °C. Immediately prior to use,

the HFIP-treated aliquots were resuspended to 5 mM in anhydrous dimethyl sulfoxide.

2.2.2. Aβ (1-42) oligomer- and fibril-forming conditions

Aβ (1-42) oligomers were prepared by diluting 5 mM Aβ (1-42) in DMSO to 100 μM in ice-cold cell culture medium Neurobasal and HCSS immediately vortexing for 30 s, and incubating at 4 °C for 24 h (Stine et al., 2003). Aβ (1-42) fibrils were prepared by diluting 5 mM Aβ (1-42) in DMSO to 100 μM in 10 mM HCl, immediately vortexing for 30 s, and incubating at 37 °C for 24 h (Stine et al., 2003).

2.2.3. Analysis of $A\beta_{oligo}$ by atomic force microscopy and Western blotting analysis

Samples containing $A\beta_{oligo}$ were prepared for AFM analysis by spotting 10 μl of solution onto freshly cleaved mica (Ted Pella, Inc., Redding, CA). Protein was allowed to adhere to the surface for 10 min at RT and then washed 2× with ddH2O to reduce background and eliminate salts and buffer contaminants. Analysis by atomic force microscopy was performed in tapping mode on the Nanoscope III (Digital Instruments, Santa Barbara, CA) equipped with a Super-SharpSiliconTM cantilever (Nanoworld AG, Neuchatel, Switzerland). Composition of $A\beta_{oligo}$ was further analyzed using Western blotting analysis with anti-amyloid antibody WO2 (The Genetics Company Inc., Zurich, Switzerland) following SDS-treatment and separation on 4–12% Nu-PAGE gel (Invitrogen, Belgium).

2.3. Calcium measurements and immunocytochemistry in primary neuronal cultures

Primary cortical and hippocampal cultures were derived from E18-embryo's of wild type mice (FVB/N background) as described previously (Dewachter et al., 2007). Intracellular calcium measurements were performed at DIV10-12. For immunocytochemistry, primary neuronal cultures were incubated during 30 min with oligomeric amyloid peptides Aβ (1-42) (100 nM) ($A\beta_{oligo}$). After two washes in PBS neurons were fixed in 4%PFA at RT during 20 min. Double-immunohistochemical staining was performed with Pan-Aβanti-Amyloid antibody (Ab-1, Oncogene Research products, San Diego, CA) followed by anti-NR2B antibody (Ab109) (Abcam, Cambridge, UK) in permeabilizing conditions (PBS with 0.1% TX-100). Alexa-488 and Alexa-594 coupled secondary antibodies (Molecular Probes, Invitrogen, CA), or alternatively chromogenic substrates, DAB and Vector SG were used for detection. It must be noted that the Pan-Aβanti-Amyloid antibody (Ab-1, Oncogene Research products, San Diego, CA) displays a very distinct staining pattern (i.e. a punctuated staining pattern and staining of amyloid plaques) as compared to anti-APP antibodies detecting the N-terminal or C-terminal part of APP, which display a more diffuse (not punctuated) cytoplasmic and dendritic/axonal staining pattern. For double-immunohistochemical staining of brain sections (vibratome sections 40 μm) of APP[V717I] × PS1[A246E] transgenic mice, immunohistochemical staining was performed using standard protocols (Dewachter et al., 2002) and using Pan-Aβanti-Amyloid antibody (Ab-1, Oncogene Research products, San Diego, CA) followed by anti-NR2B antibody (Ab109) (Abcam, Cambridge, UK).

For calcium measurements, primary neuronal cultures were incubated during 30 min with $A\beta_{oligo}$ (100 nM). $[Ca^{2+}]_i$ was measured with a monochromator-based imaging system consisting of a Polychrome IV monochromator (Till Photonics, Martinsried, Germany) and a Roper Scientific charge-coupled device camera connected to an Axiovert 200 M inverted microscope (Zeiss, Göttingen, Germany). Monochromator and camera were controlled by Metafluor software (West Chester, PA). Primary neuronal cultures were loaded with Fura-2 by incubating them for 30 min in a standard extracellular solution containing 2 μM Fura-2 acetoxymethyl ester. Fluorescence was measured during alternative excitation at 340 and 380 nm and corrected for the individual background fluorescence. The difference in the ratio of the fluorescence at both excitation wavelengths (F340/F380) before and after NMDA stimulation was calculated per neuron and statistically analyzed by single factor ANOVA.

2.4. Electrophysiology

2.4.1. Hippocampal slices

Hippocampal slices were bathed in artificial CSF containing (in mM): 124 NaCl, 5 KCl, 26 $NaHCO_3$, 1.24 KH_2PO_4, 2.4 $CaCl_2$, 1.3 $MgSO_4$, 10 glucose, aerated with 95% O_2 and 5% CO_2. Mice were anaesthetized with ether and decapitated, and transverse slices (400 μm thick) were cut in cold artificial CSF using a vibratome and kept at room temperature until placed in the interface recording chamber at 30 °C. Electrophysiological recordings were begun not earlier than 3 h after dissection to allow recovery of the slice. The chamber was perfused with artificial CSF (1 ml/min). Bipolar tungsten microelectrodes (World Precision Instruments, Sarasota, FL) were used to stimulate Schaffer's collaterals, and evoked field EPSPs (fEPSPs) were recorded in the stratum radiatum of the CA1 region with low resistance (2 MΩ) glass microelectrodes filled with 2 M NaCl. Test stimuli were 0.1 msec constant-voltage pulses delivered every 30 s at an intensity sufficient to evoke an ∼33% maximal response. LTP was induced by electrical high-frequency stimulation at an intensity evoking a 50% maximal response. The slope of the fEPSP (millivolts per millisecond) was measured from the average wave from four consecutive responses. NMDAR responses were recorded in ACSF in the presence of 20 μM CNQX. AMPAR responses were calculated as total responses minus NMDAR responses. AMPAR and NMDAR responses were measured at increasing stimulation intensity ranging from 2 to 12 V.

2.4.2. Autaptic hippocampal neurons

Autaptic hippocampal neurons were cultured as described previously (Priller et al., 2007). Whole-cell recordings on

autaptic hippocampal neurons were performed on in vitro days (DIV) 12–15 using an Axopatch-1D amplifier (Axon Instruments) at room temperature. The standard extracellular medium contained (in mM): 140 NaCl, 2.4 KCl, 10 HEPES, 10 glucose, 4 $CaCl_2$, 4 $MgCl_2$ and 15 μM bicuculline, 300 mOsm, pH 7.3. NMDA-EPSCs were measured at 4 mM external Ca^{2+} in the presence of 5 μM 6-cyano-7-nitroquinoxaline-2, 3-dione (CNQX), 10 μM glycine and in the absence of external Mg^{2+}. Internal pipette recording solution consisted of (in mM): 110 K-methanesulfonate, 5 $MgCl_2$, 10 NaCl, 40 HEPES, 0.6 EGTA, 2 MgATP, 0.3 Na_3GTP. Cells were voltage-clamped at −70 mV except for 1 ms depolarizations to 0 mV to elicit action potentials. Data were filtered at 1–2 kHz and acquired at 2–5 kHz using Igor software (Wavemetrics). All chemicals were obtained from Sigma unless specifically noted otherwise. Miniature EPSC analysis was performed manually using Synaptosoft software with an amplitude threshold of 5 pA.

2.4.3. Xenopus oocytes

The expression plasmids for rat NR1-1a and NR2A subunits and the mouse NR2B subunit have been previously described (Paoletti et al., 1997). Xenopus oocytes expressing either NR1/NR2A or NR1/NR2B were prepared, injected, voltage-clamped, and superfused as described (Paoletti et al., 1997). The standard solution superfusing the oocytes contained (in mM): 100 NaCl, 5 HEPES, 0.3 $BaCl_2$, and 10 tricine, pH was adjusted to 7.3 with KOH. NMDA currents were induced by simultaneous application of saturating concentrations of glycine and L-glutamate (100 μM each) and recorded at −60 mV.

2.5. Biochemical analysis of postsynaptic density proteins

Biochemical analysis of postsynaptic density proteins was performed as described previously (Dewachter et al., 2007). Briefly, postsynaptic densities (PSDs) were isolated from mouse brains and separated from other synaptic elements based on insolubility in the detergent Triton X-100, using a standard protocol (Carlin et al., 1980) with minor modifications. Cerebrum of age- and sex-matched APP[V717I] and non-transgenic mice ($n = 12$ for each genotype) (5 months old) was used. Brains of two mice were pooled and homogenized in 8 ml of ice-cold 0.32 M sucrose containing protease inhibitors (Amersham) and phosphatase inhibitors (NaF, sodium *ortho*-vanadate, okadaic acid) using a glass-Teflon homogenizer. Protease and phosphatase inhibitors were included in all buffers. The resulting homogenate was centrifuged at 800 × *g* for 10 min. The supernatant was pelleted again at 9200 × *g* for 15 min, and the resulting crude synaptosomal pellet was resuspended in buffer B (0.32 M sucrose and 1 mM HEPES), loaded onto a sucrose density gradient containing 15 ml each of 1.4 and 1.0 M sucrose, and centrifuged at 82,500 × *g* for 60 min in a Beckman SW 28 rotor. The band between 1.4 and 1.0 sucrose was collected and diluted in buffer B to a volume of 10 ml. After adding an equal volume of 1% (v/v) Triton X-100, the suspension was stirred for 15 min at 4 °C and centrifuged at 32,800 × *g* for 10 min. The resulting pellet was resuspended in buffer B and loaded on another sucrose density gradient containing 5 ml of 2.0 M sucrose, 3 ml of 1.5 M sucrose and 3 ml of 1.0 M sucrose. After centrifugation at 201,800 × *g* for 120 min in the Beckman SW 40 rotor, the PSD fraction band between 1.5 and 2.0 M sucrose was collected, diluted in buffer B to a volume of 1.2 ml, mixed with an equal volume of 1% Triton X-100 in 150 mM KCl and centrifuged at 113,500 × *g* for 10 min. The resulting pellet containing PSDs was collected in 20 mM HEPES buffer.

For analysis of protein concentrations in total brain homogenates, cerebrum of one hemisphere of 5 months old APP[V717I] and non-transgenic mice was homogenized in 6.5 vol of ice-cold buffer containing 20 mmol/l Tris–HCl (pH 8.5) containing a cocktail of proteinase inhibitors (Roche, Darmstadt, Germany) and phosphatase inhibitors (NaF, sodium *ortho*-vanadate, okadaic acid). After centrifugation at 135,000 × *g* at 4 °C for 1 h, pellets were resuspended in Tris-buffered saline containing protease inhibitors (Amersham) and phosphatase inhibitors (NaF, sodium *ortho*-vanadate, okadaic acid). Proteins were denatured and reduced by heating (95 °C, 5 min) in sodium dodecyl sulfate-sample buffer (final 2% sodium dodecyl sulfate, 1% 2-mercaptoethanol) and separated on 4–12% NU-PAGE or Tris–glycine gels. Western blotting was performed using anti-NR2B (Ab109), anti-PSD-95 (Ab13552), anti-α-CaMKII (phospho T286) (Ab2724) antibody (Abcam Ltd., Cambridge, UK), and home-made rabbit polyclonal anti-LRP antibody F36/4, raised against the C-terminus of LRP, for detection of the respective proteins. Densitometric scanning of films and normalization were performed using a diluted sample series as described previously (Dewachter et al., 2002, 2007; Moechars et al., 1999). Normalization was performed to LRP, a protein present in the postsynaptic density, as well as (in a similar analysis) to a non-specific protein band detected with the LRP antibody, to correct for potential protein loading differences. Concentrations of LRP and the non-specific protein band were not significantly different in PSDs derived from APP[V717I] and non-transgenic mouse brain, and therefore used for normalization of protein loading. Both normalizations yielded similar results, demonstrating decreased normalized concentrations of NR2B, PSD-95 and α-CaMKII in postsynaptic densities extracted form brain of APP[V717I] transgenic mice as compared to non-transgenic mice.

2.6. Surface biotinylation of NR2B in primary neuronal cultures

Following pre-incubation (30 min) of primary hippocampal neurons with $A\beta_{oligo}$ (300 nM) (or control medium), neurons were placed on ice, rinsed in ice-cold PBS and incubated in buffer containing 0.5 mg/ml sulfo-NHS-LC-biotin

(Pierce) (supplemented with $A\beta_{oligo}$ (300 nM) or without) for 15 min at 4 °C. Neurons were rinsed twice in PBS containing 50 mM NH_4Cl and subsequently lysed in 600 μl DIP buffer (PBS with 0.1% SDS, 1% Triton X-100, with complete proteinase inhibitor (Roche)). Cell lysates (80%) were incubated with streptavidin agarose overnight. After rinsing (four times), proteins were denaturated and reduced by boiling for 10 min in sample buffer (2% SDS, 1% BME final). Proteins were subsequently loaded on a 4–12% MES-SDS NuPAGE, and immunoblotted with anti-NR2B antibody (Abcam 109). Quantitation was performed by densitometric scanning.

2.7. Quantitation of NR2B-IR spine density in primary neuronal cultures

Following pre-incubation of primary hippocampal neurons with $A\beta_{oligo}$ (300 nM), neurons were rinsed in PBS, and processed for immuncytochemistry with anti-NR2B antibody (Ab109) (Abcam, Cambridge, UK), followed by Alexa-594 coupled secondary antibodies (Molecular Probes, Invitrogen, CA). Quantitation of NR2B-immunoreactive spine density was performed on control and $A\beta_{oligo}$ (300 nM) treated neurons ($n = 3$ dishes each). Neurons were randomly selected per dish, and for each neuron two to three dendritic segments were selected used to determine NR2B-immunoreactive spine density and length. Microscopic images were recorded and digitalized with a 3 CCD color video camera, and analyzed with dedicated software (Leica QWin Standard V2.8; Leica, Cambridge, UK). NR2B-IR spines were counted manually and were defined as protrusions that could be differentiated from the dendritic shaft and restricted to those that were visible in the *x*- and *y*-axes. Spine density was calculated by dividing the number of NR2B-IR spines per measured dendrite length.

2.8. Analysis of c-Fos induction following training in fear conditioning test

Behavioral tests were performed conforming with the Society of Animal Experimentation policy. Mice expressing mutant APP[V717I] under control of the Thy1 promoter and non-transgenic littermates were used (Moechars et al., 1999); for each line, naïve animals were used as controls while the other groups were trained ($n = 4$–5). Fear conditioning experiments were performed in a standard fear conditioning chamber with a grid floor connected to a current shocker (Med. Associates, Inc., St. Albans, VT). Freezing was quantified automatically using a video-based conditioned fear testing system, FreezeFrame (Actimetrics Software, Evanston, IL). Animals were placed in the shock chamber: at 60, 210 and 360 s, they received electric shocks (2 s, 0.5 mA, with extra light) always proceeded by 28 s of noise (tone of 3000 frequency). Forty-five minutes after the end of training, they were replaced for 5 min in the chamber and the tone was presented during 3 min. Finally, the animals were sacrificed 60 min after the end of training and perfused for immunocytochemistry.

Immunohistochemical analysis: Perfusion of the brains and c-Fos detection were performed as described elsewhere (Filipkowski et al., 2000; Savonenko et al., 2003). Briefly, mice were anesthetized with an overdose of chloral hydrate and immediately perfused with ice-cold saline followed by 4% paraformaldehyde in PBS, pH 7.4. The brains were removed and stored in the same fixative at 4 °C and then in 30% sucrose with 0.02% sodium azide at 4 °C until needed. Then the appropriate parts of the brain were frozen in a heptane/dry ice bath. Coronal cryostat sections, 45 μm thick, were cut at −20 °C, washed in PBS, incubated in 0.3% H_2O_2, incubated with anti-c-Fos antibody (1:1000, Santa Cruz Biotechnology, catalogue number sc-52, Santa Cruz, CA, USA) for 48 h at 4 °C in PBS with azide (0.01%) and normal goat serum (3%). After the sections were washed in PBS with Triton X-100 (0.3%, Sigma), incubated with goat anti-rabbit biotinylated secondary antibody (1:1000, Vector Laboratories, Burlingame, CA, USA) in PBS/Triton and normal goat serum (3%) for 2 h, washed in PBS/Triton, incubated with avidin–biotin complex (1:1000, 1:1000, in PBS/Triton, Vector) for 1 h and washed in PBS. The immunostaining reaction was developed using the DAB tablet sets (catalogue number D-4293, Sigma) enhanced with ammonium-nickel sulphate (0.1%, Sigma). The sections were mounted on gelatin-covered slides, air-dried, dehydrated in ethanol solutions and xylene, and embedded in Entellan (Merck, Darmstadt, Germany). During immunocytochemical analysis and c-Fos counting, the experimenter was blind to genotype and treatment of the mice. The number of c-Fos-positive nuclei (c-Fos grains) was determined using ImageJ 1.32j software (NIH, USA) by dividing the number of c-Fos grains of the basolateral–lateral amygdala by the area occupied by this region whereas in the hippocampus, the number of c-Fos positive cells in CA1 region was taken. Data are presented as mean ± S.E.M. Since the data were not distributed normally, the results were transformed using Box-Cox transformation (JMP3.2.6; SAS Institute Inc.) and analyzed using Analysis of Variance (ANOVA); the significance of differences was determined using pairwise analysis.

3. Results

3.1. Impaired hippocampal CA1 LTP and NMDA-receptor function in APP[V717I] transgenic mice

APP[V717I] transgenic mice display impaired long-term potentiation in the hippocampal CA1 region (Moechars et al., 1999; Dewachter et al., 2002; Postina et al., 2004). LTP measured in APP[V717I] mice involves the modulation of NMDA-receptors since administration of 50 μM APV prevented induction of LTP in identical experimental conditions (Fig. 1A and B). To further analyze NMDA-receptor function in APP[V717I] transgenic mice we measured NMDA and

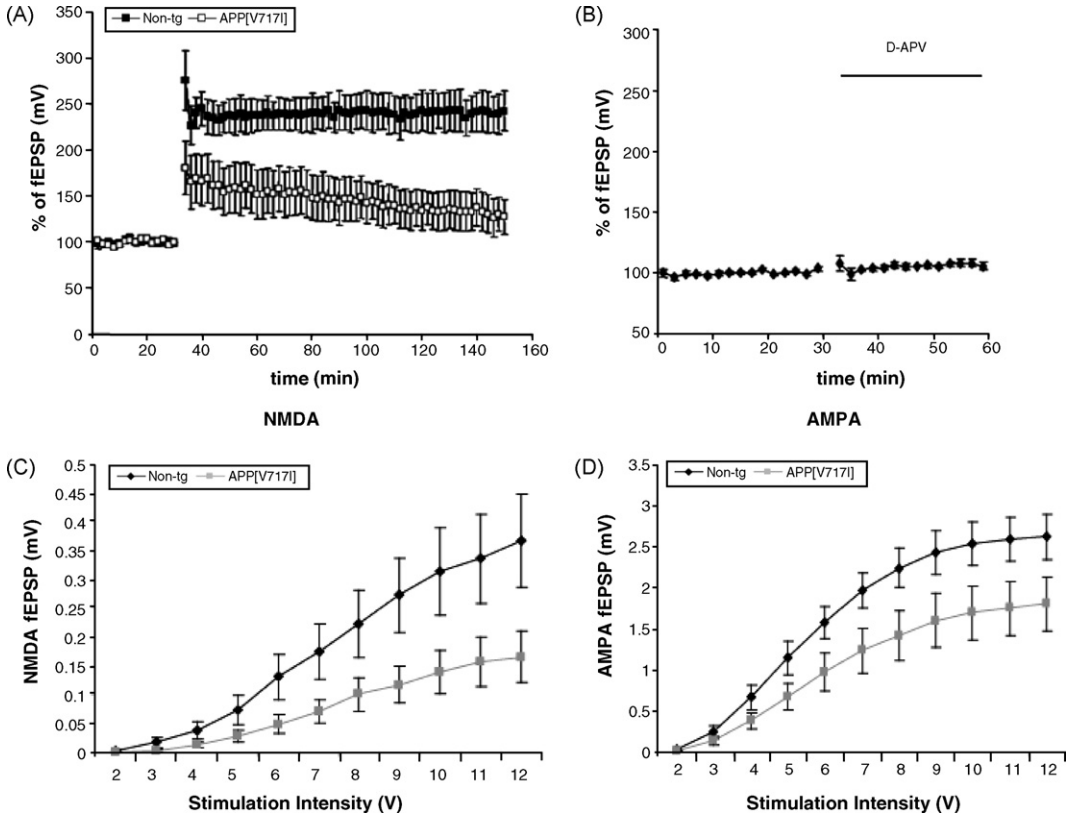

Fig. 1. NMDA-dependent long-term potentiation and NMDA-receptor responses are impaired in APP[V717I] transgenic mice. (A) The percentage of potentiation of field EPSPs recorded before and after tetanic stimulation of Schaffer's collaterals in brain slices of APP[V717I] transgenic mice and control mice. Each data point shown is the mean ± S.E.M. of results from six individual mice of each genotype. (B) Application of D-APV (50 μM) precludes induction of LTP by tetanic stimulation in the experimental conditions used for measuring LTP in APP[V717I] transgenic mice and control mice. (C and D) Plot of NMDAR-responses and AMPAR responses by the appropriate use of specific blockers, measured as extracellular fEPSP induced in APP[V717I] transgenic mice and non-transgenic mice by stimulation of the Schaffer's collaterals with increasing current intensities. This demonstrates a significant reduction in NMDAR responses (C) ($p < 0.05$ from 6 mV onwards; $n = 5$ APP[V717I] mice; $n = 5$ non-transgenic mice) and AMPAR responses (D) in CA1 in APP[V717I] mice ($p < 0.05$ from 6 mV onwards; $n = 5$ APP[V717I] mice; $n = 5$ non-transgenic mice).

AMPA receptor responses in the CA1 region of hippocampal slices. Pharmacological isolation of NMDAR responses by addition of 20 μM CNQX to the medium, revealed a significant and pronounced decrease in NMDAR responses in CA1 of APP[V717I] transgenic mice compared to non-transgenic mice (Fig. 1C). AMPA receptor responses were also reduced – albeit to a lesser extent – in hippocampal slices of APP[V717I] transgenic mice as compared to non-transgenic mice (Fig. 1D).

3.2. Amyloid peptides bind to clustered sites containing NMDA-receptor

To analyze the effect of oligomeric amyloid peptides on NMDA-receptor function, oligomeric amyloid peptides were generated and characterized as described (Stine et al., 2003). Pre-existing structures in solutions of Aβ (1-42) peptides were removed by dissolving lyophilized Aβ (1-42) in HFIP followed by evaporation of the HFIP and storage as peptide films (Stine et al., 2003). Before use, peptides were resuspended to a final concentration of 5 mM in anhydrous dimethylsulfoxide (DMSO). Oligomers were formed after dilution in cell culture medium by incubation at 4 °C during 24 h resulting predominantly in 2–8-nm oligomeric structures (Lacor et al., 2004). Atomic force microscopy confirmed the presence of small globular structures with a *z*-height ranging between 2 and 8 nm (Supplementary data, Fig. 1S). No fibrils were detected in the oligomeric amyloid peptide preparations – further denoted as $A\beta_{oligo}$ – under these conditions. Characterization of the $A\beta_{oligo}$ in SDS-PAGE revealed the presence of SDS-resistant mono-, di-, tri- and tetrameric amyloid peptides (Supplementary data, Fig. 1S).

Addition of $A\beta_{oligo}$ to cultured primary hippocampal and cortical neurons during 30 min, resulted in a specific binding pattern that exhibited abundant punctuated sites within neuronal arbors. Double staining for amyloid peptides and NMDA-receptor revealed a substantial overlap between synapses that bind $A\beta_{oligo}$ and synapses that stain for anti-NR2B (Fig. 2A–C). The incubation needed for effective binding of $A\beta_{oligo}$ to the synapses is closely in line with the timing of the impairment of synaptic plasticity in hippocampal slices (Lambert et al., 1998; Walsh et al., 2002; Dewachter et al., 2002).

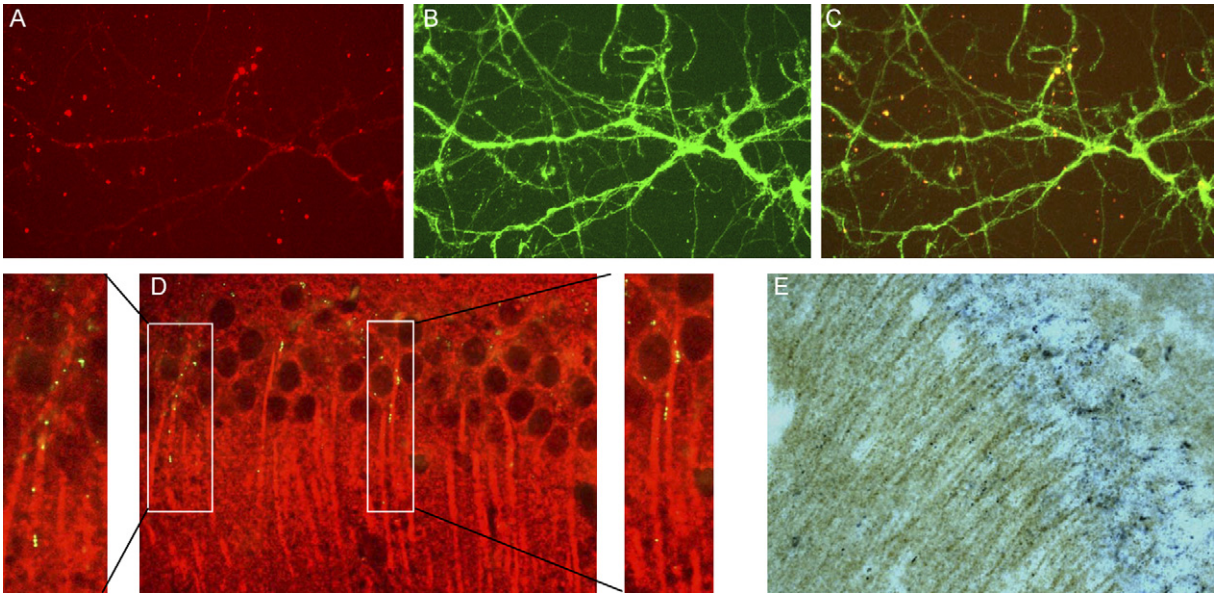

Fig. 2. Amyloid peptides substantially colocalize with NMDA-receptor subunit NR2B at synaptic contacts in primary cortical and hippocampal neurons and in vivo, in stratum radiatum of the hippocampal CA1 region. (A and C) Double-immunofluorescent staining with anti-pan β-amyloid antibody (A) and anti-NR2B (B) of primary cortical neurons, incubated with $A\beta_{oligo}$ for 30 min, reveals a substantial overlap between synapses that bind $A\beta_{oligo}$ and synapses that express NMDA-receptor subunit NR2B (merged image C). Similar results were obtained in hippocampal neurons (results not shown). (D and E) Double immunofluorescent (D) and immunohistochemical (E) staining reveal the presence of β-amyloid peptides and NMDA-receptor subunit NR2B localized in close proximity in the stratum radiatum of the hippocampal CA1 region in brain of APP[V717I] × PS1[A246E] transgenic mice, used in this experiment because of higher Aβ (1-42) concentrations. Note the abundant punctuated staining pattern following chromogenic immunohistochemical staining (E) (brown staining, DAB, NR2B), (blue staining, Vector SG, β-amyloid peptide), while fluorescent staining was less sensitive it clearly reveals colocalization (D). A higher magnification of the indicated regions is presented in the insets.

The colocalization of amyloid peptides and NMDA-receptor was further analyzed in vivo by double immunohistochemical and by double immunofluorescent staining of brain sections of old APP[V717I] × PS1[A246E] mice. Both methods demonstrate the presence of amyloid peptides in close proximity of NR2B containing NMDA-receptor in the stratum radiatum of the CA1 region of the hippocampus (Fig. 2D and E). While the immunofluorescent method was less sensitive than the immunohistochemical approach, it allowed a more clear-cut evaluation of the colocalization of amyloid peptides and the NR2B-subunit of the NMDA-receptor (Fig. 2D). Immunohistochemical staining with the Pan-Aβanti-Amyloid antibody further revealed the prominent and abundant punctuated staining in the stratum radiatum of the hippocampus in close proximity of NR2B-containing receptors (Fig. 2E).

The experimental observation of the substantial overlap between synapses that bind or contain $A\beta_{oligo}$ or amyloid peptides and synapses that express NMDA-receptors incited us to test whether ADDLs affect NMDA-receptor function directly.

3.3. Pre-incubation with amyloid peptides inhibits NMDA-receptor mediated calcium ion influx

We measured the effect of $A\beta_{oligo}$ and fibrillar amyloid peptides on NMDA-induced changes in intracellular calcium concentration ($[Ca^{2+}]_i$) in primary cortical and hippocampal neurons. Application of NMDA (100 μm) in the presence of glycine (10 μM) and in the absence of Mg^{2+}, caused a rapid increase in $[Ca^{2+}]_i$ in all neuronal cultures analyzed, which became progressively restored upon washing out the NMDA. Pre-incubation of primary hippocampal and cortical neurons with 100 nM $A\beta_{oligo}$ for 30 min, resulted in a significant attenuation of NMDA-induced $[Ca^{2+}]_i$ increase (Fig. 3). Pre-incubation of primary neuronal cultures with concentration up to 1 μM fibrillar amyloid peptides during 30 min did not attenuate NMDA-induced $[Ca^{2+}]_i$ increase (results not shown).

To analyze whether $A\beta_{oligo}$ have a direct pharmacological effect on NMDA-receptors, we analyzed the effects of acute applications of $A\beta_{oligo}$ on the NMDA currents recorded in autaptic hippocampal glutamatergic neurons. For measurements of acute effects of $A\beta_{oligo}$ using patch clamp analysis, synaptic currents were measured 5 min before the application of $A\beta_{oligo}$, throughout the application, and up to 5–7 min after the application. Acute application of $A\beta_{oligo}$ (Aβ1-42) peptides up to 1 μM did not significantly affect NMDA-EPSC amplitude nor AMPA-EPSC amplitudes (Fig. 4A and B). Moreover, no differences in spontaneous NMDA mEPSC amplitudes or frequency were detected upon acute application of $A\beta_{oligo}$ (Fig. 4C). Short-term plasticity, i.e. paired-pulse facilitation of NMDA-currents and paired-pulse depression of AMPA-currents, was not significantly changed by acute application of $A\beta_{oligo}$ (Fig. 4D and E). Also acute application of amyloid fibrils did not reveal any significant

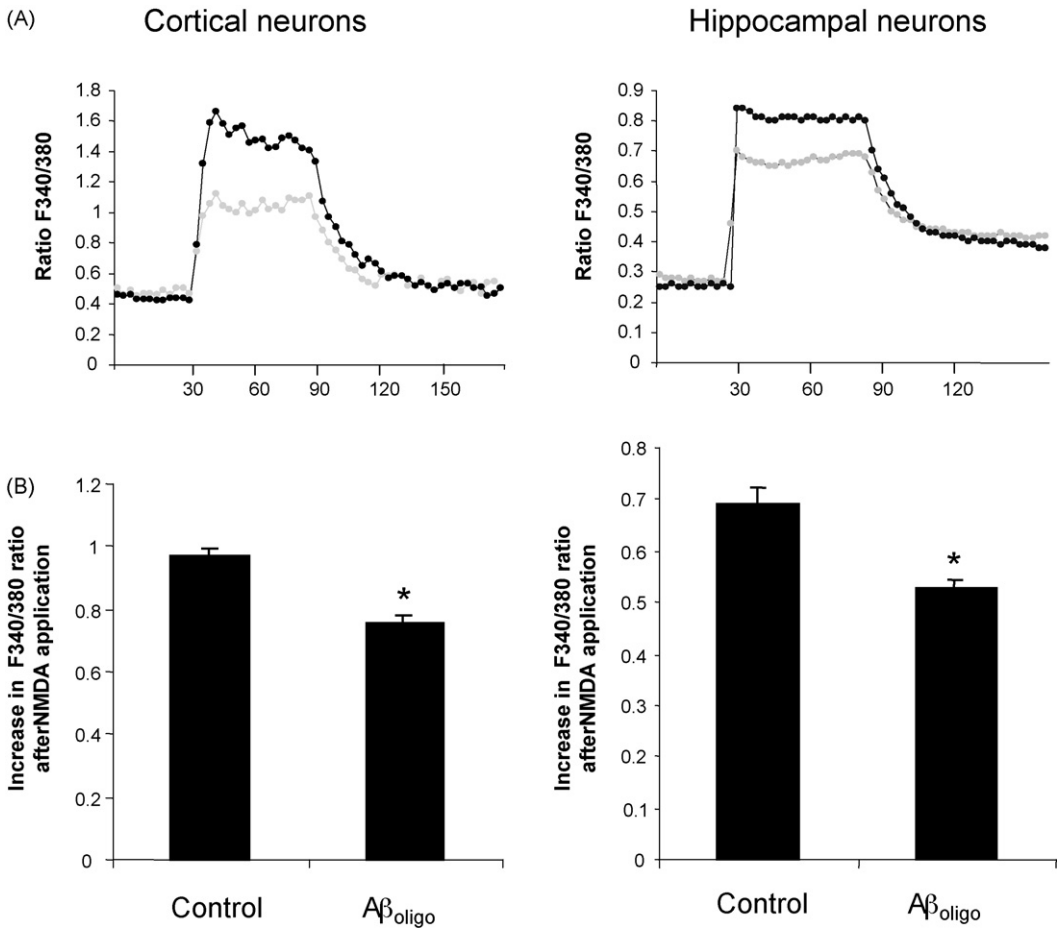

Fig. 3. NMDA-induced calcium influx is attenuated in primary hippocampal and cortical neuronal cultures following pre-incubation with $A\beta_{oligo}$. (A) Application of NMDA (100 μm) in the presence of glycine (10 μM) and the absence of Mg^{2+}, caused a rapid $[Ca^{2+}]_i$ increase in Fura-2-loaded primary hippocampal and cortical neuronal cultures, while washing out of the NMDA progressively restored $[Ca^{2+}]_i$. Representative traces of NMDA-induced increase in ratio F340/380 in primary cortical and hippocampal neurons following 30 min treatment with $A\beta_{oligo}$ (Aβ (1-42)) (100 nM) (light grey traces, light grey dots) or without (dark traces, dark dots) are presented. (B) Quantitation of NMDA-induced increase in intracellular calcium concentration in primary cortical (left panel) and hippocampal (right panel) neurons following 30 min treatment with or without $A\beta_{oligo}$ (Aβ (1-42)) peptides (100 nM). The difference between ratio F340/380 before and after application of NMDA was measured. Bars represent averages ±S.E.M. ($^{*}p < 0.05$, $n = 3$ experiments, $n = 75$ neurons for each condition).

differences in any of the parameters measured, i.e. AMPA-EPSC, spontaneous mEPSC amplitude and frequency and paired-pulse depression (Fig. 4F and G).

We also tested the effect of acute applications of $A\beta_{oligo}$ on recombinant NMDA-receptors expressed in Xenopus laevis oocytes. $A\beta_{oligo}$ were applied during the activation of NMDA-receptors by long application of glutamate and glycine (each at 100 μM). No significant change of ion currents was measured upon application of $A\beta_{oligo}$ in NR1/NR2B as well as in NR1/NR2A expressing oocytes (Fig. 5; 99 ± 2% of the current before application of $A\beta_{oligo}$, $n = 5$ for both types of receptors).

The combined data demonstrate that oligomeric amyloid peptides do not directly modulate the activation and conductance properties of native and recombinant NMDA-receptors. The need for the pre-incubation with $A\beta_{oligo}$ indicated on the other hand that the $A\beta_{oligo}$ disturbed NMDA-receptor mediated synaptic currents by other mechanisms.

3.4. Synaptic expression of NR2B containing NMDA-receptors is decreased following long-term incubation with amyloid peptides

To analyze whether $A\beta_{oligo}$ can affect synaptic expression of NMDA-receptors and thereby affect NMDA-receptor functioning, we analyzed synaptic expression of NR2B in primary hippocampal neurons following incubation with $A\beta_{oligo}$. Following pre-incubation of primary hippocampal neurons with $A\beta_{oligo}$ (300 nM), the number of NR2B-immunoreactive spines per dendrite length was significantly decreased compared to control conditions (Fig. 6A), as demonstrated by immunofluorescent staining with anti-NR2B antibody. These observations are in line with the recent demonstration of amyloid induced decrease in surface and synaptic expression of NMDA-receptors and phosphorylation of NR2B at Tyr-1472 (Snyder et al., 2005). We further confirmed decreased surface expression of NR2B following pre-incubation of primary hippocampal neurons with $A\beta_{oligo}$.

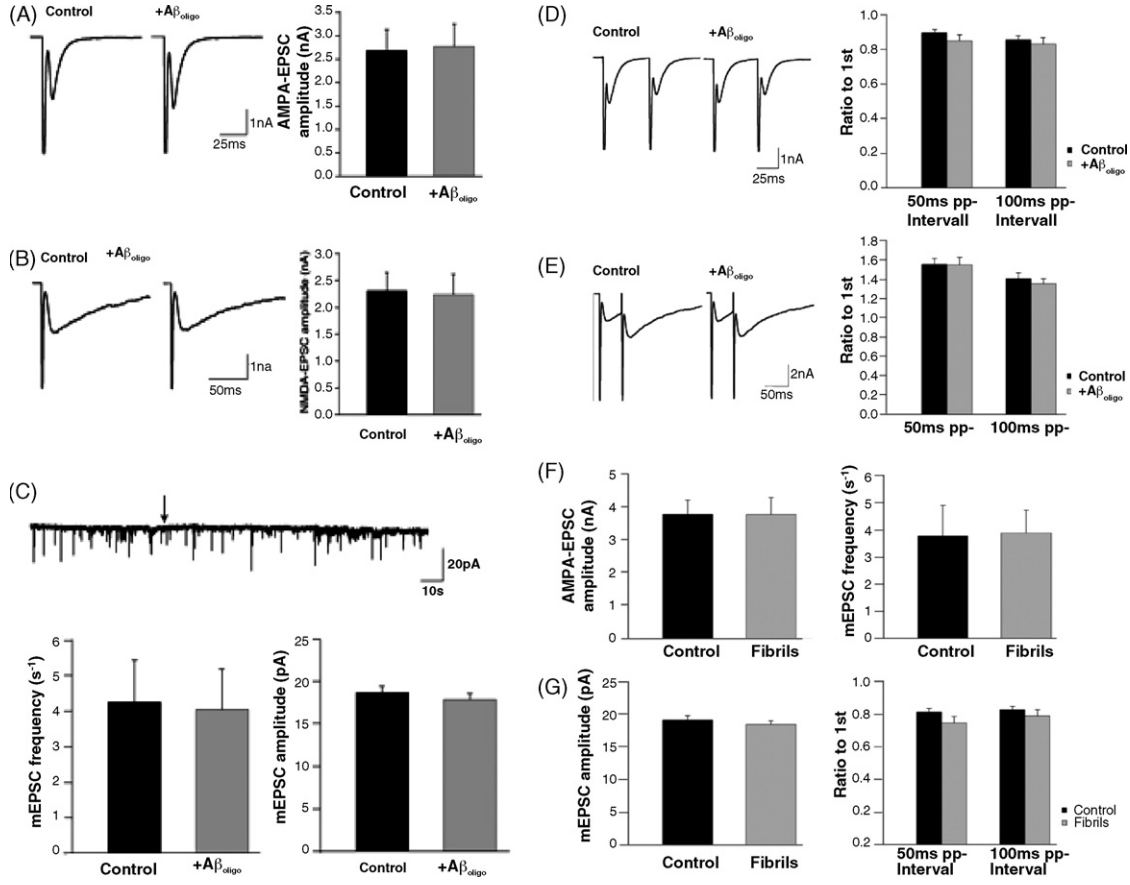

Fig. 4. No direct pharmacological effect of $A\beta_{oligo}$ on NMDA-receptor currents in primary autaptic hippocampal neurons. Evoked and spontaneous neurotransmitter release in control cells and after acute application of $A\beta_{oligo}$ (1 μM). (A) Representative AMPA-EPSC traces from control and $A\beta_{oligo}$-treated neurons (left). AMPA-EPSC amplitude in neurons from control ($n = 30$) and $A\beta_{oligo}$-treated cells ($n = 30$) (right). (B) Representative NMDA-traces from control and $A\beta_{oligo}$-treated neurons (left). NMDA-EPSC amplitude in neurons from control ($n = 14$) and $A\beta_{oligo}$-treated cells ($n = 14$) (right). (C) Representative mEPSC trace with $A\beta_{oligo}$ application after 60 s indicated by arrow. mEPSC frequency in control ($n = 27$) and $A\beta_{oligo}$-treated neurons ($n = 25$) (left) and mEPSC amplitude in control cells ($n = 27$) and after $A\beta_{oligo}$ application ($n = 25$) (right). (D and E) Paired-pulse stimulation after acute application of $A\beta_{oligo}$. (D) Representative AMPA-traces from control and $A\beta_{oligo}$-treated neurons (left) induced by paired-pulse depression. Quantification of paired-pulse depression of AMPA-currents from control ($n = 12$) and $A\beta_{oligo}$-treated neurons ($n = 19$) (right). (E) Representative NMDA-traces from control and $A\beta_{oligo}$ -treated neurons (left) induced by paired-pulse facilitation. Quantitation of paired-pulse facilitation of NMDA-currents from control ($n = 12$) and $A\beta_{oligo}$-treated cells ($n = 12$) (right). (F and G) Evoked and spontaneous neurotransmitter release and paired-pulse stimulation in control cells and after acute Aβ-fibril application (1 μM). (F) AMPA-EPSC amplitude in control ($n = 21$) and Aβ-fibril treated neurons ($n = 18$) (left) and mEPSC frequency in control cells ($n = 21$) and after Aβ-fibril application ($n = 15$) (right). (G) mEPSC amplitude in control ($n = 21$) and Aβ-fibril treated cells ($n = 15$) (left) and paired-pulse depression of AMPA-currents from control ($n = 8$) and Aβ-fibril treated cells ($n = 11$) (right).

Western blotting analysis following biotinylation demonstrated decreased ratios of the concentrations of biotinylated NR2B to total NR2B following pre-incubation with $A\beta_{oligo}$ (Fig. 6B).

3.5. Expression of postsynaptic proteins is affected in vivo in APP[V717I] transgenic mice

We next analyzed postsynaptic NMDA-receptor expression in vivo by analyzing postsynaptic densities extracted from brains of APP[V717I] transgenic mice. PSD fractions were purified from mouse brain by a protocol that is based on its resistance to solubilization by Triton X-100, consisting essentially of two sequential sucrose density gradients (Dewachter et al., 2007). Quantitative analysis of the NMDA-receptor subunit NR2B, the postsynaptic protein PSD-95 and α-CaMKII kinase phosphorylated at Thr-268, was performed on isolated PSD fractions from APP[V717I] transgenic and non-transgenic mice, and compared after normalization to the postsynaptic protein, LDL receptor-related protein (LRP). Concentrations of NR2B, PSD-95 and phosphorylated α-CaMKII were significantly lower in PSD preparations from brains of APP[V717I] transgenic mice as compared to non-transgenic mice (Fig. 6C). Concentrations of NR2B, PSD-95, phosphorylated α-CaMKII and LRP were however not significantly decreased in total brain homogenates of APP[V717I] transgenic mice as compared to non-transgenic mice, at this age (5 months old). PSD-95 is a major protein at the postsynaptic density, which binds to NMDA-receptor NR2 subunits (Sheng and Pak, 1999) and is important in anchor-

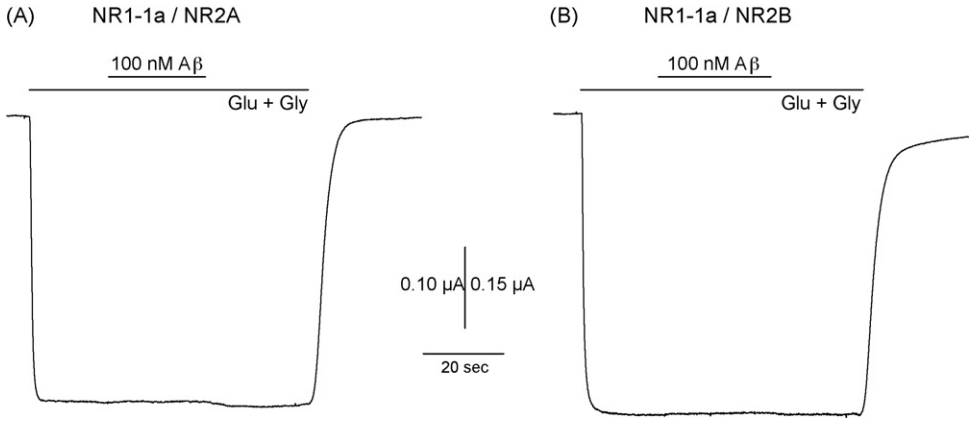

Fig. 5. No direct pharmacological inhibiton of acute $A\beta_{oligo}$ application on recombinant NMDA-receptors expressed in xenopus oocytes. No reduction of NMDA-receptor current was measured in Xenopus laevis oocytes expressing functional recombinant NR1-1a/NR2A (A) or NR1-1a/NR2B receptors (B) following acute application of $A\beta_{oligo}$ (Aβ (1-42)) (100 nM) during long application of glutamate and glycine (100 μM each); recording at −60 mV.

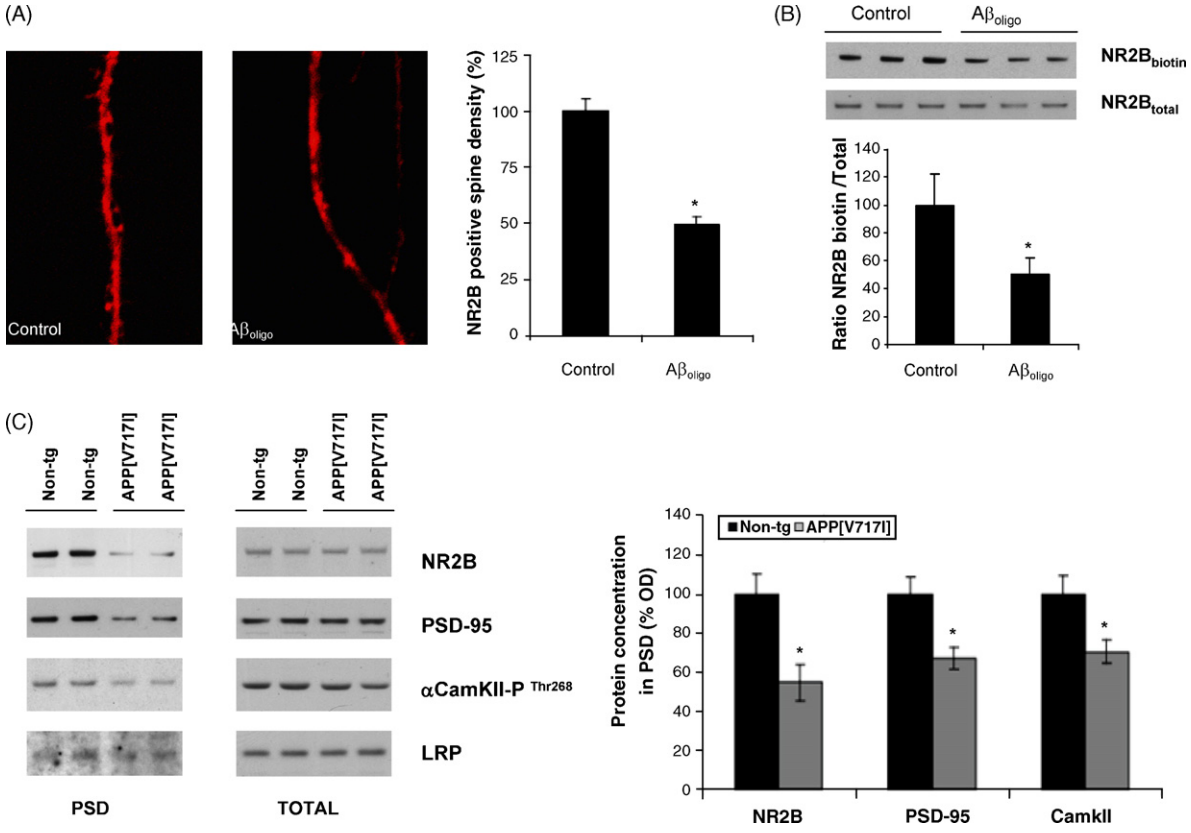

Fig. 6. Synaptic expression of NR2B containing NMDA-receptors is decreased following long-term incubation with $A\beta_{oligo}$. (A) Immunofluorescent staining of primary hippocampal neurons following incubation in control conditions or $A\beta_{oligo}$ (300 nM, 1 h), with anti-NR2B antibody, reveals a decrease in NR2B-immunoreactive dendritic spines following $A\beta_{oligo}$ treatment. Quantitation of NR2B-positive synaptic density relative to control conditions in $A\beta_{oligo}$ treated primary hippocampal cultures, reveals a significant decrease in NR2B synaptic expression ($p < 0.05$, $n = 10$ and $n = 12$ neurons for, respectively, $A\beta_{oligo}$ treatment and control conditions). (B) Surface expression of NR2B analyzed by surface biotinylation at 4 °C is significantly decreased following pre-incubation with $A\beta_{oligo}$. Quantitation of the ratio of biotinylated to total NR2B reveals a significant decrease following pre-incubation with $A\beta_{oligo}$ ($p < 0.05$, $n = 9$; $n = 8$, $A\beta_{oligo}$; control). Representative Western blots immunostaining biotinylated NR2B and total NR2B are presented in the upper panel. (C) Analysis of the concentration of postsynaptic density proteins extracted from brains of APP[V717I] mice and non-transgenic mice, reveals a significant decrease in the concentration of NR2B, PSD-95 and α-CamkII phosphorylated at Threonine 268, after normalization to LRP in APP[V717I] mice ($p < 0.05$, $n = 12$ APP[V717I] transgenic mice and $n = 12$ non-transgenic mice; brains of two mice were pooled for extraction of postsynaptic densities, Western blotting was performed in triplicate). Representative Western blots of postsynaptic density preparations are presented in the left panel. Analysis of total brain homogenates revealed no significant changes in the concentrations of NR2B, PSD-95, α-CamkII $P^{Thr\text{-}268}$ and LRP in brain of APP[V717I] mice ($n = 5$ APP[V717I] transgenic mice and $n = 5$ non-transgenic mice). Representative Western Blots of protein extracts from total brain homogenates are presented in the right panel.

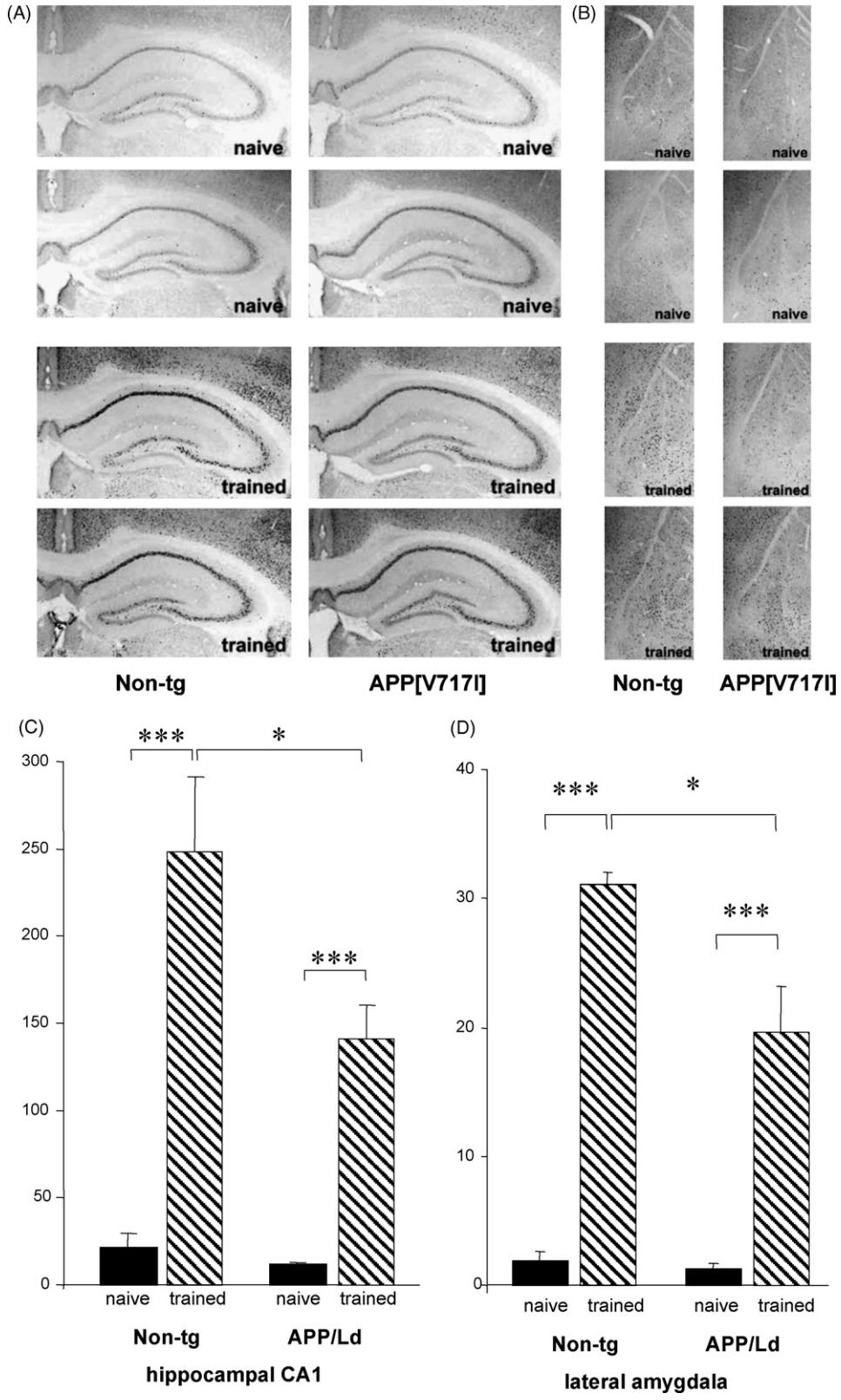

Fig. 7. Signaling pathways activated by NMDA-receptor activation are affected in the brain of APP[V717I] mice: Cued and contextual fear conditioning induced expression of c-Fos is attenuated in APP[V717I] transgenic mice. (A and B) Immunohistochemical staining of c-Fos is induced by fear conditioning training in the hippocampus (CA1 field) (A) and basolateral–lateral amygdala (B) in non-transgenic (left column) and APP[V717I] mice right column). Two representative mice from each group are shown. Note a more intense c-Fos induction in non-transgenic compared to APP[V717I] mice in hippocampus (A) and amygdale (B). (C and D) Quantitation of c-Fos immunoreactivity reveals increased c-Fos expression in both regions, however the increase in APP[V717I] mice is significantly lower as compared to non-transgenic mice in hippocampal CA1 region (C) and basolateral amygdala (D). Graphs present means ± S.E.M.; $^{*}p < 0.05$; $^{***}p < 0.001$.

ing glutamate receptors to signaling proteins and the neuronal cytoskeleton at the synapse (Hering and Sheng, 2001). In primary hippocampal neurons PSD-95 expression at the post-synaptic density is decreased before synaptic degeneration (Almeida et al., 2005). In addition, decreased concentrations of phosphorylated α-CaMKII in PSD preparations of APP[V717I] transgenic mice suggest impaired NMDA-dependent signaling in brain of APP[V717I] transgenic mice.

3.6. Signaling pathways downstream of the NMDA-receptor are disturbed in brain of APP[V717I] mice

We further extended our findings to the analysis of NMDA-dependent downstream signaling pathways involved in learning and memory. APP[V717I] and non-transgenic mice were subjected to a context- and cue-dependent fear conditioning paradigm, in which mice learn to associate a novel context (experimental chamber) or cue (auditory tone, 90 dB, 3.0 kHz, 30 s) with a foot shock (0.5 mA, 2 s) after triple pairing. Cue-dependent fear conditioning is dependent on intact amygdala, while context-dependent fear conditioning requires both hippocampus and amygdala (Maren and Holt, 2000; Maren and Quirk, 2004). Mice were sacrificed 60 min after the end of the training. Immunohistochemical analysis demonstrated that c-Fos expression was induced by the fear conditioning training in the hippocampus (CA1 field) and in the basolateral–lateral amygdala in both non-transgenic and APP[V717I] transgenic mice ($p < 0.001$) (Fig. 7). The increase in c-Fos was however much lower in the APP[V717I] mutant mice, i.e. 35% for the amygdala and 43% in CA1 ($p < 0.02$ for both) (Fig. 7). We conclude that cognitive training induced the expression of c-Fos in the CA1 region of the hippocampus as well as in the lateral-basolateral nuclei of the amygdala, but the induction of c-Fos was significantly attenuated in APP[V717I] transgenic mouse model, indicative for impaired learning-dependent signaling in APP[V717I] transgenic mice.

4. Discussion

In this study we analyzed the mechanisms involved in synaptic dysfunction in APP[V717I] transgenic mice, a mouse model that appears to mimic early cognitive impairment in the early phases in Alzheimer's Disease (Moechars et al., 1999; Dewachter et al., 2002). Transgenic mice that overexpress mutant APP display early deficits in synaptic plasticity and memory (Moechars et al., 1999; Chapman et al., 1999; Dewachter et al., 2002; Oddo et al., 2003). A crucial role for amyloid peptides in the disruption of synaptic plasticity and cognition is supported by a variety of data (Lambert et al., 1998; Moechars et al., 1999; Dewachter et al., 2002; Dodart et al., 2002; Cleary et al., 2005; Klyubin et al., 2005; Puzzo et al., 2005; Walsh et al., 2005a,b; Lesne et al., 2006; Gong et al., 2006; Snyder et al., 2005, for reviews see Selkoe, 2002; Walsh and Selkoe, 2004; Walsh et al., 2005a,b; Small et al., 2001; Small, 2004), while the mechanisms involved remain unclear. Our current data provide a combined in vitro and in vivo analysis, which contribute to the understanding of mechanisms involved in synaptic defects in APP transgenic mice, in vivo.

We here demonstrate that NMDA-dependent long-term potentiation and NMDA- and AMPA-dependent excitatory synaptic transmission is significantly impaired in hippocampal CA1 region of APP[V717I] transgenic mice. Our findings thereby extend previous reports demonstrating impaired AMPA- and NMDA-dependent synaptic transmission by viral expression of mutant APP in organotypic hippocampal cultures (Kamenetz et al., 2003), to APP transgenic mice. To further analyze the mechanisms involved in NMDA-receptor dysfunction we used a combined in vitro and in vivo analysis. Incubation of primary neuronal cultures with $A\beta_{oligo}$ resulted in a punctuated synaptic staining pattern that substantially overlapped with NR2B synaptic staining in hippocampal and cortical neuronal cultures. These data are in line with previous reports demonstrating that amyloid peptides bind to a subset of synaptic terminals on excitatory but not inhibitory neurons (Lacor et al., 2004, 2007). It must be noted that Aβ exists in several different physical states, including monomers, insoluble fibrils as well as soluble oligomers, which further comprise small SDS-resistant oligomers, including di-, tri-, tetramers, and dodecamers (Lesne et al., 2006; Oddo et al., 2003; Walsh et al., 2002). The preparation of $A\beta_{oligo}$ used in the present study consisted of a non-fibrillar Aβ preparation, comprising oligomeric amyloid peptides, which after SDS-treatment are detected as monomers and di-, tri-, and tetramers on Western Blot. Small SDS-resistant oligomers have previously been shown to potently inhibit LTP following 45–60 min pre-incubation in hippocampal slices (Lambert et al., 1998; Wang et al., 2002; Klyubin et al., 2005). Our in vitro data were further extended in vivo, demonstrating colocalization of anti-amyloid stained puncta and anti-NR2B staining in the stratum radiatum of the hippocampal CA1 region, a region displaying decreased NMDA-receptor dependent synaptic transmission.

Our data further indicate that $A\beta_{oligo}$ impaired NMDA-receptor function, most probably not by a direct pharmacological inhibition but rather by affecting synaptic expression of NMDA-receptors. Pre-incubation of primary neuronal cultures with $A\beta_{oligo}$ significantly impaired NMDA-induced calcium influx. In contrast, direct application of $A\beta_{oligo}$ did not affect NMDA-receptor currents in primary autaptic neurons, nor in xenopus oocytes overexpressing recombinant NMDA-receptors. The analysis of a direct pharmacological effect of amyloid peptides is not only fundamentally important, but is also therapeutically relevant. The slow effects on NMDA-receptor functions are proposed to be exerted by affecting synaptic surface expression of NMDA-receptors containing NR2B subunit. Because pre-incubation of primary neuronal cultures with $A\beta_{oligo}$ resulted in decreased NR2B reactive spine density and decreased NR2B surface expres-

sion as revealed by biotinylation. These data are consistent with previous data demonstrating that amyloid peptides affect surface NMDA-receptor expression in vitro, in primary neuronal cultures (Snyder et al., 2005; Lacor et al., 2007). Accumulating evidence supports the hypothesis that amyloid peptides affect synapse composition and structure (Lacor et al., 2007) and can drive loss of surface glutamate receptors, i.e. NMDA- and AMPA-receptors as well as molecules involved in the anchoring of these receptors in the postsynaptic membrane, like PSD-95 (Snyder et al., 2005; Almeida et al., 2005; Hsieh et al., 2006; Goto et al., 2006; Lacor et al., 2007). Our data confirm the published in vitro data, but importantly these data are now extended, for the first time in vivo by demonstrating changes in composition of the postsynaptic density, i.e. decreased NR2B and PSD-95 expression in APP[V717I] transgenic mice.

The exact molecular mechanisms underlying the changes induced by amyloid on NMDA-receptor expression in postsynaptic densities, and other synaptic proteins, remain unclear. Amyloid peptides may interact with neuronal membranes by non-specific associations or by pore-formation (Kayed et al., 2004). Alternatively, they can bind more specifically to particular membrane targets as effective ligands (Lacor et al., 2004, 2007). Amyloid peptides bind with high affinity to alpha7 nicotinic acetylcholine receptors (Wang et al., 2000; Dineley et al., 2001) while ADDLs bind selectively to synaptic targets that are present in the postsynaptic density but are yet to be identified (Lacor et al., 2004, 2007). These interactions have been proposed to deregulate ion homeostasis and signaling cascades downstream the nicotinic acetylcholine receptor or other pathways (Vitolo et al., 2002; Wang et al., 2004; Puzzo et al., 2005). Amyloid peptides affect NMDA-receptor trafficking, eventually mediated by alpha-7 nicotinic receptors and modulation of PP2B and STEP, resulting in tyrosine phosphorylation of NR2B and affecting NR2B expression (Snyder et al., 2005, and references therein).

Amyloid peptides have been implicated in several other signaling cascades, i.e. inhibition of the PKA/CREB pathway and activation of the nitric oxide/cGMP/cAMP-responsive element-binding protein pathway (Vitolo et al., 2002; Puzzo et al., 2005). Pharmacological studies suggested roles for several kinases in amyloid induced LTP impairment, including p38MAPK (p38 mitogen-activated protein kinase), JNK (c-Jun N-terminal protein kinase), and cdk5 (cyclin-dependent kinase 5) (Wang et al., 2004).

Recently, amyloid peptides were reported to employ signaling pathways of LTD (like calcineurin and p38 MAP kinase activity) to drive endocytosis of AMPA-receptors, a process sufficient to produce loss of dendritic spines (Hsieh et al., 2006; Shankar et al., 2007). While deregulation of kinases and phosphatases might directly affect the phosphorylation of NMDA-receptor and its surface expression, also indirect effects might contribute like deregulation of glutamate receptor anchoring proteins (e.g. PSD-95), proteins interacting with glutamate receptors (e.g. EphB-receptor) or proteins associated with the actin-cytoskeleton like drebrin, spinophilin. Furthermore, ADDLs have been reported to induce abnormal expression of the immediate early gene Arc (activity-regulated cytoskeletal-associated) protein (Lacor et al., 2004). Arc protein is a synaptic F-actin coupled and memory-related protein, in a manner predicted to cause abnormal spine shape and receptor trafficking (Lacor et al., 2004, 2007).

It follows that the exact sequence of events leading from amyloid to decreased NMDA-receptor expression remains unclear and that the exact contribution of the above mentioned mechanisms, their hierarchy of actions, parallel or sequential, are all to be determined in detail. It must however be concluded that amyloid peptide induced synaptic loss does involve NMDA-receptor dysfunction (Lacor et al., 2007; Shankar et al., 2007), indicating that this is an "early" event in the amyloid induced synaptic changes. Our in vitro data presented here are in line with the published data, which are extended now in vivo and correlated to electrophysiological, behavioral and biochemical analyses.

Long-term potentiation in the hippocampal CA1 region has been intensely studied as a mechanism of learning and memory at the cellular level, yielding a detailed insight in the molecular mechanisms involved. Recently, the functional link between long-term potentiation, the best studied form of synaptic plasticity, and memory became corroborated by the demonstration of LTP in vivo in a hippocampus dependent learning task (Whitlock et al., 2006). LTP in hippocampal CA1 can be initiated by Ca^{2+} entry through NMDA-receptors (Bliss and Collingridge, 1993). NMDA-dependent Ca^{2+} influx thereby triggers a biochemical cascade that includes the activation of α-CaMKII by phosphorylation at Threonine 268 and translocation to the postsynaptic density and eventually the activation of immediate early genes (IEGs) like c-Fos (Fleischmann et al., 2003). Activation of signaling pathways following NMDA-receptor activation or tetanic stimulation was demonstrated to be disrupted by soluble Aβ oligomers in vitro (Vitolo et al., 2002; Snyder et al., 2005; Puzzo et al., 2005; Almeida et al., 2005), but analysis of the signaling cascades that are deregulated by amyloid peptides in vivo is lacking. In hippocampus and amygdala the immediate early gene c-Fos is induced following training in a variety of learning tasks (Miyamoto, 2006; Tischmeyer and Grimm, 1999), while c-Fos deficiency impairs memory (Fleischmann et al., 2003). Several studies demonstrated association between NMDA-receptor activity and c-Fos regulation in different models of synaptic plasticity (Cole et al., 1989; Herrera and Robertson, 1990; Aronin et al., 1991) as well as in long-term memory formation (Fleischmann et al., 2003; Savonenko et al., 2003) (for reviews, Kaczmarek and Chaudhuri, 1997; Platenik et al., 2000; Kaczmarek, 2002). We here report for the first time decreased concentrations of activated and translocated α-CamkII in postsynaptic densities of APP[V717I] transgenic mice. Moreover, training in the fear conditioning paradigm impaired the induction of c-Fos protein in the hippocampus, and to a lesser extent in the amygdala of APP[V717I] transgenic mice, indicating that

the induction of immediate early genes by learning induced NMDA-dependent signaling cascades is deregulated also in vivo.

In summary, our data demonstrate that $A\beta_{oligo}$ affect NMDA-receptor function, and suggest no direct pharmacological inhibitory effect on NMDA-receptors, but indicate that $A\beta_{oligo}$ rather contribute to synaptic failure by affecting synaptic expression of NMDA-receptor subunit NR2B and other synaptic proteins. We furthermore report decreased NMDA-receptor and AMPA-receptor responses in APP[V717I] transgenic mice in hippocampal CA1 region, correlating with colocalization of NR2B and amyloid peptides in this region. The functional changes were further associated with decreased expression of NR2B, PSD-95 and activated α-CamKII in the postsynaptic densities in brains of APP[V717I] transgenic mice. Finally the changes in NMDA-receptor function and expression were associated with deregulation of learning induced signaling cascades as induction of c-Fos following fear conditioning was significantly impaired in hippocampus and amygdala of APP[V717I] transgenic mice. Our data yield insight in the mechanisms involved in synaptic plasticity in vivo in APP[V717I] transgenic mice, a model that mimics the early stages of Alzheimer's Disease. We believe that a complete understanding of the early phases of AD, characterized by early synaptic defects is not only fundamentally important but is also absolutely required for the development of therapeutic strategies that aim at curing AD at a stage that the damage is still reversible. Our data thereby gain insight in the mechanisms involved in early synaptic dysfunction, one of the most important targets for AD therapy.

Conflicts of interest

There are no actual or potential conflicts of interest including any financial, personal or other relationships with other people or organizations within three years of beginning the work submitted that could inappropriately influence their work.

Disclosure statement

No author's institution has contracts relating to this research through which it or any other organization may stand to gain financially now or in the future.

There are no other agreements of authors of their institutions that could be seen as involving a financial interest in this work. The data contained in the manuscript being submitted have not been submitted elsewhere and will not be submitted elsewhere while under consideration at Neurobiology of Aging. All authors have reviewed the contents of the manuscript being submitted, approved of its contents and validated the accuracy of the data.

Acknowledgements

All experiments with animals were performed in accordance with the regulations of, and authorized by the Ethical Commission for Animal Experimentation of the K.U.Leuven. This work was supported by the DFG (SFB 596) and the Bayerische Forschungsverbunt ForPrion. R.K.F. and L.K. were supported by Polish MNSW Scientific Network fund and UE QLRT-2001-02775 grant. This investigation was made possible by funding and support from the Fonds voor Wetenschappelijk Onderzoek-Vlaanderen (FWO-Vlaanderen), the Instituut voor Wetenschappelijk en Technologisch onderzoek (IWT), the EEC-6th Framework Program, the Rooms-fund, the K.U.Leuven Special Research Fund (BOF - GOA) and K.U.Leuven-R&D. I.D. is senior post-doctoral fellow at FWO-Vlaanderen., L.R. is a Research Associate of the Belgian National Fund for Scientific Research (NFSR). L.R. and E.G. were supported by NFSR and the Queen Elisabeth Fund for Medical Research.

Appendix A. Supplementary data

Supplementary data associated with this article can be found, in the online version, at doi:10.1016/j.neurobiolaging.2007.06.011.

References

Almeida, C.G., Tampellini, D., Takahashi, R.H., Greengard, P., Lin, M.T., Snyder, E.M., Gouras, G.K., 2005. Beta-amyloid accumulation in APP mutant neurons reduces PSD-95 and GluR1 in synapses. Neurobiol. Dis. 20 (2), 187–198.

Aronin, N., Chase, K., Sagar, S.M., Sharp, F.R., DiFiglia, M., 1991. N-methyl-D-aspartate receptor activation in the neostriatum increases c-fos and fos-related antigens selectively in medium-sized neurons. Neuroscience 44, 409–420.

Bliss, T.V., Collingridge, G.L., 1993. A synaptic model of memory: long-term potentiation in the hippocampus. Nature 361, 31–39.

Carlin, R.K., Grab, D.J., Cohen, R.S., Siekevitz, P., 1980. Isolation and characterization of postsynaptic densities from various brain regions: enrichment of different types of postsynaptic densities. J. Cell Biol. 86, 831–843.

Chapman, P.F., White, G.L., Jones, M.W., Cooper-Blacketer, D., Marshall, V.J., Irizarry, M., Younkin, L., Good, M.A., Bliss, T.V., Hyman, B.T., Younkin, S.G., Hsiao, K.K., 1999. Impaired synaptic plasticity and learning in aged amyloid precursor protein transgenic mice. Nat. Neurosci. 2 (3), 271–276.

Cleary, J.P., Walsh, D.M., Hofmeister, J.J., Shankar, G.M., Kuskowski, M.A., Selkoe, D.J., Ashe, K.H., 2005. Natural oligomers of the amyloid-beta protein specifically disrupt cognitive function. Nat. Neurosci. 8 (1), 79–84.

Cole, A.J., Saffen, D.W., Baraban, J.M., Worley, P.F., 1989. Rapid increase of an immediate early gene messenger RNA in hippocampal neurons by synaptic NMDA receptor activation. Nature 340, 474–476.

Dewachter, I., Van Dorpe, J., Smeijers, L., Gilis, M., Kuiperi, C., Laenen, I., Caluwaerts, N., Moechars, D., Checler, F., Vanderstichele, H., Van Leuven, F., 2000. Aging increased amyloid peptide and caused amyloid plaques in brain of old APP/V717I transgenic mice by a different mechanism than mutant presenilin1. J. Neurosci. 20 (17), 6452–6458.

Dewachter, I., Reverse, D., Caluwaerts, N., Ris, L., Kuiperi, C., Van den Haute, C., Spittaels, K., Umans, L., Serneels, L., Thiry, E., Moechars, D., Mercken, M., Godaux, E., Van Leuven, F., 2002. Neuronal deficiency of presenilin 1 inhibits amyloid plaque formation and corrects hippocampal long-term potentiation but not a cognitive defect of amyloid precursor protein [V717I] transgenic mice. J. Neurosci. 22 (9), 3445–3453.

Dewachter, I., Ris, L., Croes, S., Borghgraef, P., Devijver, H., Voets, T., Nilius, B., Godaux, E., Van Leuven, F., 2008. Modulation of synaptic plasticity and Tau phosphorylation by wild-type and mutant presenilin1. Neurobiol. Aging 29, 639–652.

Dineley, K.T., Westerman, M., Bui, D., Bell, K., Ashe, K.H., Sweatt, J.D., 2001. Beta-amyloid activates the mitogen-activated protein kinase cascade via hippocampal alpha7 nicotinic acetylcholine receptors: In vitro and in vivo mechanisms related to Alzheimer's disease. J. Neurosci. 21 (12), 4125–4133.

Dodart, J.C., Bales, K.R., Gannon, K.S., Greene, S.J., DeMattos, R.B., Mathis, C., DeLong, C.A., Wu, S., Wu, X., Holtzman, D.M., Paul, S.M., 2002. Immunization reverses memory deficits without reducing brain Abeta burden in Alzheimer's disease model. Nat. Neurosci. 5 (5), 452–457.

Filipkowski, R.K., Rydz, M., Berdel, B., Morys, J., Kaczmarek, L., 2000. Tactile experience induces c-fos expression in rat barrel cortex. Learn. Mem. 7 (2), 116–122.

Fleischmann, A., Hvalby, O., Jensen, V., Strekalova, T., Zacher, C., Layer, L.E., Kvello, A., Reschke, M., Spanagel, R., Sprengel, R., Wagner, E.F., Gass, P., 2003. Impaired long-term memory and NR2A-type NMDA receptor-dependent synaptic plasticity in mice lacking c-Fos in the CNS. J. Neurosci. 23 (27), 9116–9122.

Gong, Y., Chang, L., Viola, K.L., Lacor, P.N., Lambert, M.P., Finch, C.E., Krafft, G.A., Klein, W.L., 2003. Alzheimer's disease-affected brain: presence of oligomeric A beta ligands (ADDLs) suggests a molecular basis for reversible memory loss. Proc. Natl. Acad. Sci. U.S.A. 100 (18), 10417–10422.

Gong, B., Cao, Z., Zheng, P., Vitolo, O.V., Liu, S., Staniszewski, A., Moolman, D., Zhang, H., Shelanski, M., Arancio, O., 2006. Ubiquitin hydrolase Uch-L1 rescues beta-amyloid-induced decreases in synaptic function and contextual memory. Cell 126 (4), 775–788.

Goto, Y., Niidome, T., Akaike, A., Kihara, T., Sugimoto, H., 2006. Amyloid beta-peptide preconditioning reduces glutamate-induced neurotoxicity by promoting endocytosis of NMDA receptor. Biochem. Biophys. Res. Commun. 351 (1), 259–265.

Hering, H., Sheng, M., 2001. Dendritic spines: structure, dynamics and regulation. Nat. Rev. Neurosci. 2, 880–888.

Herrera, D.G., Robertson, H.A., 1990. N-methyl-D-aspartate receptors mediate activation of the c-fos proto-oncogene in a model of brain injury. Neuroscience 35, 273–281.

Hsieh, H., Boehm, J., Sato, C., Iwatsubo, T., Tomita, T., Sisodia, S., Malinow, R., 2006. AMPAR removal underlies Abeta-induced synaptic depression and dendritic spine loss. Neuron 52 (5), 831–843.

Kaczmarek, L., 2002. c-Fos in learning: beyond the mapping of neuronal activity. In: Immediate Early Genes and Inducible Transcription Factors in Mapping of the Central Nervous System Function and Dysfunction, In: Kaczmarek, L., Robertson, H.A. (Eds.), Handbook of Chemical Neuroanatomy, vol. 19. Elsevier, Amsterdam, Boston, London, New York, Oxford, Paris, San Diego, San Francisco, Singapore, Sydney, Tokyo, pp. 189–216.

Kaczmarek, L., Chaudhuri, A., 1997. Sensory regulation of immediate-early gene expression in mammalian visual cortex: implications for functional mapping and neural plasticity. Brain Res. Brain Res. Rev. 23, 237–256.

Kamenetz, F., Tomita, T., Hsieh, H., Seabrook, G., Borchelt, D., Iwatsubo, T., Sisodia, S., Malinow, R., 2003. APP processing and synaptic function. Neuron 37 (6), 925–937.

Kayed, R., Sokolov, Y., Edmonds, B., McIntire, T.M., Milton, S.C., Hall, J.E., Glabe, C.G., 2004. Permeabilization of lipid bilayers is a common conformation-dependent activity of soluble amyloid oligomers in protein misfolding diseases. J. Biol. Chem. 279 (45), 46363–46366.

Klyubin, I., Walsh, D.M., Lemere, C.A., Cullen, W.K., Shankar, G.M., Betts, V., Spooner, E.T., Jiang, L., Anwyl, R., Selkoe, D.J., Rowan, M.J., 2005. Amyloid beta protein immunotherapy neutralizes Abeta oligomers that disrupt synaptic plasticity in vivo. Nat. Med. 11 (5), 556–561.

Lacor, P.N., Buniel, M.C., Chang, L., Fernandez, S.J., Gong, Y., Viola, K.L., Lambert, M.P., Velasco, P.T., Bigio, E.H., Finch, C.E., Krafft, G.A., Klein, W.L., 2004. Synaptic targeting by Alzheimer's-related amyloid beta oligomers. J. Neurosci. 24 (45), 10191–10200.

Lacor, P.N., Buniel, M.C., Furlow, P.W., Clemente, A.S., Velasco, P.T., Wood, M., Viola, K.L., Klein, W.L., 2007. Abeta oligomer-induced aberrations in synapse composition, shape, and density provide a molecular basis for loss of connectivity in Alzheimer's disease. J. Neurosci. 27 (4), 796–807.

Lambert, M.P., Barlow, A.K., Chromy, B.A., Edwards, C., Freed, R., Liosatos, M., Morgan, T.E., Rozovsky, I., Trommer, B., Viola, K.L., Wals, P., Zhang, C., Finch, C.E., Krafft, G.A., Klein, W.L., 1998. Diffusible, nonfibrillar ligands derived from Abeta1-42 are potent central nervous system neurotoxins. Proc. Natl. Acad. Sci. U.S.A. 95 (11), 6448–6453.

Lesne, S., Koh, M.T., Kotilinek, L., Kayed, R., Glabe, C.G., Yang, A., Gallagher, M., Ashe, K.H., 2006. A specific amyloid-beta protein assembly in the brain impairs memory. Nature 440 (7082), 352–357.

Maren, S., Holt, W., 2000 Jun. 1. The hippocampus and contextual memory retrieval in Pavlovian conditioning. Behav. Brain Res. 110 (1–2), 97–108.

Maren, S., Quirk, G.J., 2004 Nov. Neuronal signalling of fear memory. Nat. Rev. Neurosci. 5 (11), 844–852.

Miyamoto, E., 2006. Molecular mechanism of neuronal plasticity: induction and maintenance of long-term potentiation in the hippocampus. J. Pharmacol. Sci. 100 (5), 433–442 (Review).

Moechars, D., Dewachter, I., Lorent, K., Reverse, D., Baekelandt, V., Naidu, A., Tesseur, I., Spittaels, K., Van den Haute, C., Checler, F., Godaux, E., Cordell, B., Van Leuven, F., 1999. Early phenotypic changes in transgenic mice that overexpress different mutants of amyloid precursor protein in brain. J. Biol. Chem. 274 (10), 6483–6492.

Oddo, S., Caccamo, A., Shepherd, J.D., Murphy, M.P., Golde, T.E., Kayed, R., Metherate, R., Mattson, M.P., Akbari, Y., LaFerla, F.M., 2003. Triple-transgenic model of Alzheimer's disease with plaques and tangles: intracellular Abeta and synaptic dysfunction. Neuron 39 (3), 409–421.

Paoletti, P., Ascher, P., Neyton, J., 1997. High-affinity zinc inhibition of NMDA NR1–NR2A receptors. J. Neurosci. 17, 5711–5725.

Platenik, J., Kuramoto, N., Yoneda, Y., 2000. Molecular mechanisms associated with long-term consolidation of the NMDA signals. Life Sci. 67, 335–364.

Postina, R., Schroeder, A., Dewachter, I., Bohl, J., Schmitt, U., Kojro, E., Prinzen, C., Endres, K., Hiemke, C., Blessing, M., Flamez, P., Dequenne, A., Godaux, E., Van Leuven, F., Fahrenholz, F., 2004. A disintegrin-metalloproteinase prevents amyloid plaque formation and hippocampal defects in an Alzheimer disease mouse model. J. Clin. Invest. 113 (10), 1456–1464.

Priller, C., Dewachter, I., Vassallo, N., Paluch, S., Pace, C., Kretzschmar, H.A., Van Leuven, F., Herms, J., 2007. Mutant presenilin 1 alters synaptic transmission in cultured hippocampal neurons. J. Biol. Chem. 282 (2), 1119–1127.

Puzzo, D., Vitolo, O., Trinchese, F., Jacob, J.P., Palmeri, A., Arancio, O., 2005. Amyloid-beta peptide inhibits activation of the nitric oxide/cGMP/cAMP-responsive element-binding protein pathway during hippocampal synaptic plasticity. J. Neurosci. 25 (29), 6887–6897.

Savonenko, A., Werka, T., Nikolaev, E., Zielinski, K., Kaczmarek, L., 2003. Complex effects of NMDA receptor antagonist APV in the basolateral amygdala on acquisition of two-way avoidance reaction and long-term fear memory. Learn. Mem. 10, 293–303.

Selkoe, D.J., 2002. Alzheimer's disease is a synaptic failure. Science 298 (5594), 789–791 (Review).

Shankar, G.M., Bloodgood, B.L., Townsend, M., Walsh, D.M., Selkoe, D.J., Sabatini, B.L., 2007. Natural oligomers of the Alzheimer amyloid-beta protein induce reversible synapse loss by modulating an NMDA-type glutamate receptor-dependent signaling pathway. J. Neurosci. 27 (11), 2866–2875.

Sheng, M., Pak, D.T., 1999. Glutamate receptor anchoring proteins and the molecular organization of excitatory synapses. Ann. N.Y. Acad. Sci. 868, 483–493.

Small, D.H., 2004. Mechanisms of synaptic homeostasis in Alzheimer's disease. Curr. Alzheimer Res. 1 (1), 27–32 (Review).

Small, D.H., Mok, S.S., Bornstein, J.C., 2001. Alzheimer's disease and Abeta toxicity: from top to bottom. Nat. Rev. Neurosci. 2 (8), 595–598 (Review).

Snyder, E.M., Nong, Y., Almeida, C.G., Paul, S., Moran, T., Choi, E.Y., Nairn, A.C., Salter, M.W., Lombroso, P.J., Gouras, G.K., Greengard, P., 2005. Regulation of NMDA receptor trafficking by amyloid-beta. Nat. Neurosci. 8 (8), 1051–1058.

Stine Jr., W.B., Dahlgren, K.N., Krafft, G.A., LaDu, M.J., 2003. In vitro characterization of conditions for amyloid-beta peptide oligomerization and fibrillogenesis. J. Biol. Chem. 278 (13), 11612–11622.

Tischmeyer, W., Grimm, R., 1999. Activation of immediate early genes and memory formation. Cell Mol. Life Sci. 55 (4), 564–574 (Review).

Van Dorpe, J., Smeijers, L., Dewachter, I., Nuyens, D., Spittaels, K., Van Den Haute, C., Mercken, M., Moechars, D., Laenen, I., Kuiperi, C., Bruynseels, K., Tesseur, I., Loos, R., Vanderstichele, H., Checler, F., Sciot, R., Van Leuven, F., 2000. Prominent cerebral amyloid angiopathy in transgenic mice overexpressing the london mutant of human APP in neurons. Am. J. Pathol. 157 (4), 1283–1298.

Vitolo, O.V., Sant'Angelo, A., Costanzo, V., Battaglia, F., Arancio, O., Shelanski, M., 2002. Amyloid beta -peptide inhibition of the PKA/CREB pathway and long-term potentiation: reversibility by drugs that enhance cAMP signaling. Proc. Natl. Acad. Sci. U.S.A. 99 (20), 13217–13221.

Walsh, D.M., Klyubin, I., Fadeeva, J.V., Cullen, W.K., Anwyl, R., Wolfe, M.S., Rowan, M.J., Selkoe, D.J., 2002. Naturally secreted oligomers of amyloid beta protein potently inhibit hippocampal long-term potentiation in vivo. Nature 416 (6880), 535–539.

Walsh, D.M., Selkoe, D.J., 2004. Deciphering the molecular basis of memory failure in Alzheimer's disease. Neuron 44 (1), 181–193 (Review).

Walsh, D.M., Townsend, M., Podlisny, M.B., Shankar, G.M., Fadeeva, J.V., Agnaf, O.E., Hartley, D.M., Selkoe, D.J., 2005a. Certain inhibitors of synthetic amyloid beta-peptide (Abeta) fibrillogenesis block oligomerization of natural Abeta and thereby rescue long-term potentiation. J. Neurosci. 25 (10), 2455–2462.

Walsh, D.M., Klyubin, I., Shankar, G.M., Townsend, M., Fadeeva, J.V., Betts, V., Podlisny, M.B., Cleary, J.P., Ashe, K.H., Rowan, M.J., Selkoe, D.J., 2005b. The role of cell-derived oligomers of Abeta in Alzheimer's disease and avenues for therapeutic intervention. Biochem. Soc. Trans. 33 (Pt 5), 1087–1090, Review.

Wang, H.W., Pasternak, J.F., Kuo, H., Ristic, H., Lambert, M.P., Chromy, B., Viola, K.L., Klein, W.L., Stine, W.B., Krafft, G.A., Trommer, B.L., 2002. soluble oligomers of beta amyloid (1-42) inhibit long-term potentiation but not long-term depression in rat dentate gyrus. Brain Res. 924 (2), 133–140.

Wang, H.Y., Lee, D.H., D'Andrea, M.R., Peterson, P.A., Shank, R.P., Reitz, A.B., 2000. beta-Amyloid (1-42) binds to alpha7 nicotinic acetylcholine receptor with high affinity. Implications for Alzheimer's disease pathology. J. Biol. Chem. 275 (8), 5626–5632.

Wang, Q., Walsh, D.M., Rowan, M.J., Selkoe, D.J., Anwyl, R., 2004. Block of long-term potentiation by naturally secreted and synthetic amyloid beta-peptide in hippocampal slices is mediated via activation of the kinases c-Jun N-terminal kinase, cyclin-dependent kinase 5, and p38 mitogen-activated protein kinase as well as metabotropic glutamate receptor type 5. J. Neurosci. 24 (13), 3370–3378.

Whitlock, J.R., Heynen, A.J., Shuler, M.G., Bear, M.F., 2006. Learning induces long-term potentiation in the hippocampus. Science 313 (5790), 1093–1097.